

# Combustion and Emission Characteristics of Premixed and Non-premixed Ammonia/air Turbulent Swirl Flames at the High Pressure and Temperature

K.D.Kunkuma A. Somarathne, Akihiro Hayakawa and Hideaki Kobayashi  
Tohoku University  
Sendai, Miyagi, Japan

## 1 Introduction

Sustainable solutions are needed to be increasingly applied to the energy sector in order to prevent the detrimental effects of fossil fuels on the environment. Ammonia ( $\text{NH}_3$ ) is, recently, identified as a carbon free sustainable fuel, and anticipated as a hydrogen energy carrier because of the higher hydrogen capacity of 17.8% in weight. Nevertheless, much lower laminar burning velocity [1-2] and high fuel NO generation in the combustion, because  $\text{NH}_3$  contains nitrogen itself than that of conventional hydrocarbon fuels, hindered the use of  $\text{NH}_3$  as a commercial fuel. However, recent studies of Somarathne et al. [3-4] and Hayakawa et al. [5] have numerically and experimentally illustrated that by introducing swirl flow, and thereby making a recirculation near the downstream of swirler,  $\text{NH}_3$ /air turbulent premixed flames have successfully achieved a stable combustion at the atmospheric pressure and various turbulent intensities at the initial mixture temperature of 500 K and 300 K. Moreover, the studies of [3-5] elucidated that fuel NO generation can be significantly reduced by using the rich flame condition and there is an equivalence ratio in rich flame condition in which NO and unburnt  $\text{NH}_3$  emissions are minimal and in a same order, and thus, this would be the best operating point for the selective catalytic NO emission reduction (SCR) process in the downstream. However, this specific equivalence ratio like to be depended on the initial mixture temperature and burner wall condition, and in the case of adiabatic wall and initial mixture temperature of 300 K and 500 K, the equivalence ratios were 1.15 and 1.2, [3-4] respectively, whereas in the case of isothermal wall and initial mixture temperature of 300 K, the specific equivalence ratio is 1.05 [5].

In addition, recently,  $\text{NH}_3$ /air combustion power generation has been successfully realized using a 50 kW micro gas turbine at the National Institute of Advanced Science and Technology (AIST), Japan by Kurata et al. [6]. In the study of [6], stable turbulent non-premixed ammonia/air swirl flame has been achieved using a high swirling flow of air and a jet flow of  $\text{NH}_3$ , nevertheless NO and unburnt  $\text{NH}_3$  emissions are still higher than that of the government environment regulations [7]. However, insights of the combustion and emission characteristics of non-premixed  $\text{NH}_3$ /air flames in gas turbine combustors are still unclear. Besides, to the best of author's knowledge, there is no any comprehensive study on turbulent  $\text{NH}_3$ /air flames at high

Correspondence to: [kunkuma@flame.ifs.tohoku.ac.jp](mailto:kunkuma@flame.ifs.tohoku.ac.jp)

pressures, which is essential for the design of the gas turbine combustors. There are only few numerical studies on one-dimensional (1D) laminar NH<sub>3</sub>/air premixed flames at high pressures. Duynslaegher et al. [8] showed that the increase in the pressure leads to decrease NO emission, and Hayakawa et al. [9] illustrated that the third body reaction of  $\text{OH} + \text{H} + \text{M} \rightleftharpoons \text{H}_2\text{O} + \text{M}$  plays an important role in reduction of NO emission at the high pressures.

Thus, the present study is dedicated to understand the combustion and emission characteristics of turbulent premixed and non-premixed NH<sub>3</sub>/air swirl flames at high pressures and temperatures. Accordingly, a relative simple test cases were chosen as affordable tests to evaluate the feasibilities of more complex gas turbine combustors. Because of gas turbine combustor modeling comprise a wide range computational and modeling challenges owing to the involvement of the interactions of many complex physical process such as turbulence-chemistry interaction, in the present study, large eddy simulation (LES) with a finite rate chemistry is performed in a three-dimensional computational domain.

## 2 Numerical Models and Conditions

In the present study, spatially filtered Navier-Stokes equations were used, and the reacting flow simulations were conducted using the open-source code, OpenFOAM at the supercomputer center of the Institute of Fluid science, Tohoku University, Japan. In the spatially filtered momentum equation, the unresolved subgrid scale tensor is modeled by wall adapting local eddy-viscosity (WALE) subgrid scale model [10], and, in addition, unresolved fluxes of species and sensible enthalpy of spatially filtered mass fraction and sensible enthalpy equations are described as a gradient assumption. Even though the laminar burning velocity estimation has a slightly over prediction than experimental measurements [2], the Miller's chemical kinetics [11], which consists of 23-species and 98-elementary reactions, for the NH<sub>3</sub> oxidation was selected in this study by considering the computational burden of other detailed mechanisms. An *in-situ* adaptive tabulation algorithm library was used to calculate the composition changes through chemical reaction, and thereby reduce the computational burden.

The unstructured three dimensional computational domain, which was used for the high pressure NH<sub>3</sub>/air premixed flames, is same as the study of [3]. The domain consists of the cylindrical combustion chamber, which was installed vertically, and an annulus swirl burner was installed at the center of bottom of the combustion chamber. The inner and outer diameters,  $D_i$  and  $D_o$  of the swirler were 14 mm and 24 mm, respectively. The chamber had inner diameter of 72 mm ( $= 3D_o$ ), and a height of 150 mm. The circular outflow channel, which was placed on the top of the cylinder, had an inner diameter of 36 mm ( $= 1.5 D_o$ ) and length of 10 mm. The swirler flow inlet was located 1 mm upstream from the bottom of the chamber. The swirler angle,  $\alpha$ , was approximately 40 degree, and accordingly, the swirler number,  $S$ , was 0.68.

Table 1: Initial operating conditions

Combustion Type	Premixed			Non-Premixed					
$P_0$ [MPa]	0.1, 0.2, 0.5			0.1, 0.5					
$\phi$ / overall $\phi$	1.0, 1.25, 1.4		1.0	1.1	1.2	1.25			
$U_{in}$ [m/s]	NH <sub>3</sub> /air	NH <sub>3</sub>	air	NH <sub>3</sub>	air	NH <sub>3</sub>	air	NH <sub>3</sub>	air
	39.1	31.27	30.53	33.45	29.93	35.60	29.33	36.70	29.03

On the other hand, for the simulation cases of the high pressure non-premixed flames, the dimensions of cylindrical combustion chamber is the same as the premixed cases. In addition, the swirler, which was used for NH<sub>3</sub>/air mixture in the premixed cases, was used for the swirling flow of air, and thereby  $S_{\text{air}} = S$ . Moreover, NH<sub>3</sub> flow passed through a new inner swirler, which was located inside to the air swirler, and has inner and outer diameters of 8 mm and 13 mm, respectively, and, in this case, fuel-swirler angle,  $\alpha_{\text{NH}_3}$ , was also same as air-swirler angle,  $\alpha_{\text{air}} = \alpha$ , and thereby  $S_{\text{NH}_3} = 0.69$ .

In all the cases, the temperature at the inlet flow was 500 K, total volumetric flow rate is 0.009 m<sup>3</sup>/s, and the relative turbulent intensity of 30 % was set for the all inlet flows in order to retain a higher turbulent intensity in the flow field. In addition, LES characteristics length scale in the flow field is approximately 0.63 mm, which corresponds to an approximately cubic root of a computational cell of 0.25 mm<sup>3</sup>. The operating conditions, in terms of operating pressure,  $P_0$ , equivalence ratio,  $\phi$ , and mean velocity at the inlet,  $U_{\text{in}}$ , are shown in Table 1. The origin of the coordinates was set at the center of the bottom of the combustion chamber, and the axial and radial coordinates are indicated by  $z$  and  $r$ , respectively.

### 3 Results and Discussion

**Reacting flow fields:** In the present study, the instantaneous reacting flow field of premixed turbulent NH<sub>3</sub>/air flame at  $\phi = 1$  and  $P_0 = 0.5$  MPa is briefly discussed by means of the streamlines in a vertical plane of the combustion chamber and iso-surfaces of the second invariant of the velocity gradient tensor,  $Q$ , at  $3 \times 10^7$  (selected as a median value), which is shaded by the mass fraction of NH<sub>3</sub>,  $Y_{\text{NH}_3}$ , as shown in Figs. 1 (a) and (b). In the reacting flow field an inner recirculation zone (IRZ) strongly associate with the vortex breakdown bubble owing to the lower pressure of backside in the swirling flow, whereas an outer recirculation zone (ORZ) generated by the rapid expansion of the annular swirling flow into the combustion chamber as shown in Fig. 1(a). The rotational flow structure of the swirling flow is clearly shown in Fig. 1 (a) by means of the iso-surfaces of the second invariant of the velocity gradient tensor at  $Q = 3 \times 10^7$ . Here, iso-surfaces are shaded according to the mass fraction of NH<sub>3</sub>, and it helps to determine the flame length indirectly.

**Flame structure of the premixed flames:** Figure 2 illustrates the flame structures of the premixed turbulent NH<sub>3</sub>/air flames at  $\phi = 1.0$  and 1.25 in terms of  $P_0$  using the temperature distributions, and, in the Fig. 2, temperature profiles show the almost uniform temperature distributions in the flame region. In addition,

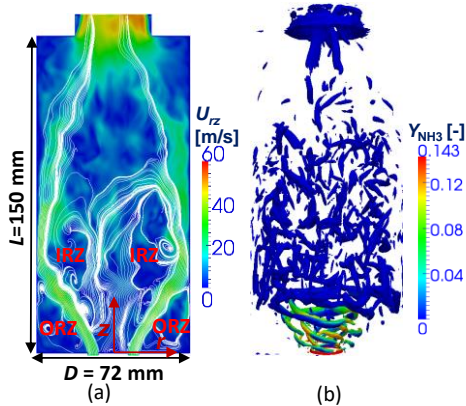


Figure 1. Instantaneous reacting flow field of turbulent premixed NH<sub>3</sub>/air flames at  $\phi = 1$  and  $P_0 = 0.5$  MPa.

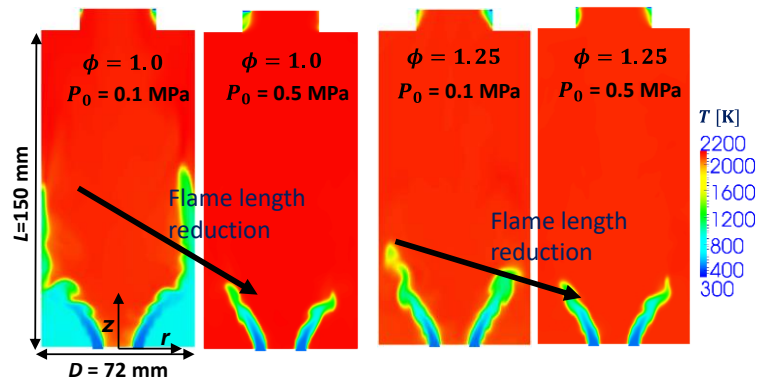


Figure 2. Temperature distributions of turbulent premixed NH<sub>3</sub>/air flames at  $\phi = 1.0$  and 1.25 in terms of  $P_0$ .

more significantly observed that the increase in the operating pressure leads to the reduction of the flame length of premixed flames irrespective to the equivalence ratio. Possibly this may associate with the considerable reduction of the chemical reaction time scale,  $\tau_c$ , with increase in pressure, especially between the  $P_0$  of 0.1 MPa and 0.5 MPa, as shown in Fig. 3. Here  $\tau_c = \alpha_{th}/S_L^2$ , and  $\alpha_{th}$  and  $S_L$  donate the thermal diffusivity and laminar burning velocity, respectively, and calculated by 1D flame model using CHEMKIN-PRO. The shorter  $\tau_c$  at elevated pressures leads to the enhancement of the reaction rate, and thereby, reduction of flame length.

**Effect of the pressure on NO emission of premixed flames:** The NO and OH distributions at  $P_0$  of 0.1 and 0.5 MPa are shown in Figs. 4(a) and (b), respectively, at  $\phi = 1$ . The space and time averaged emission (SATE) of NO,  $x_{NO}$ , was calculated at the exit of the combustion chamber and shown in Fig. 4 (a). Moreover, hereafter  $X_k$  and  $x_k$  denote the mole fraction of species  $k$  and SATE of  $k$ , respectively. The increase in operating pressure leads to the decrease in NO production, and consequently, NO emission at  $P_0$  of 0.5 MPa is nearly half of that of 0.1 MPa. Simultaneously, it was observed that there is a significant reduction of OH concentration at  $P_0$  of 0.5 MPa than that of 0.1 MPa as shown in Fig. 4 (b). As pointed out by Miller et al. [12], OH radicals play an important role when amidogen (NH<sub>2</sub>) is oxidized to NO through nitroxyl (HNO) by the reaction sequence ( $\text{HNO} + \text{OH} \rightleftharpoons \text{NO} + \text{H}_2\text{O}$ ), and hence, the reduction of OH concentration in the high pressure by the third body reaction of  $\text{OH} + \text{H} + \text{M} \rightleftharpoons \text{H}_2\text{O} + \text{M}$  leads to the reduction of NO emission at the high pressures. However, the impact of pressure on emission reduction of NO is minimal at the rich flame condition (significantly  $\phi > 1.2$ ), as shown in Fig. 9 (the later part of the abstract), because of lower OH concentration even at the 0.1 MPa owing to the lower temperature and O<sub>2</sub> deficiency.

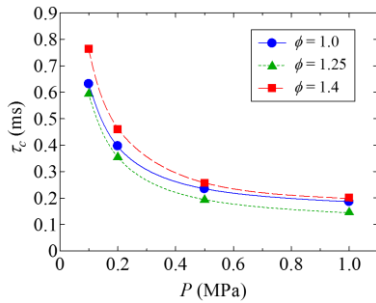


Figure 3. Effect of pressure on the chemical characteristic time scale in terms of  $\phi$

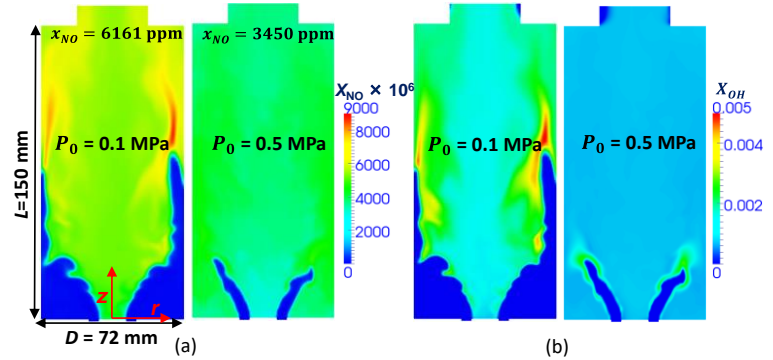


Figure 4. Effect of pressure on : (a) NO concentration; (b) OH concentration; at  $\phi = 1$ .

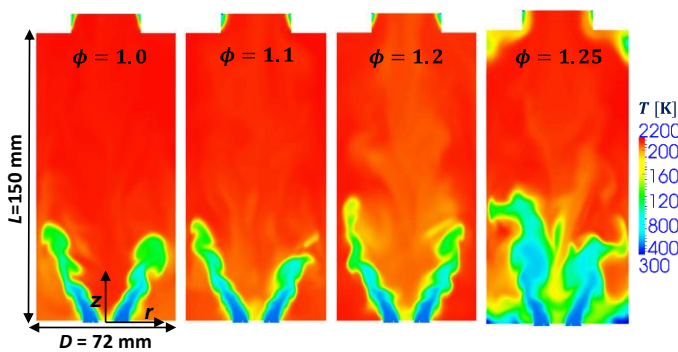


Figure 5. Temperature distributions of non-premixed NH<sub>3</sub>/air flames at  $P_0 = 0.1$  MPa in terms of overall  $\phi$

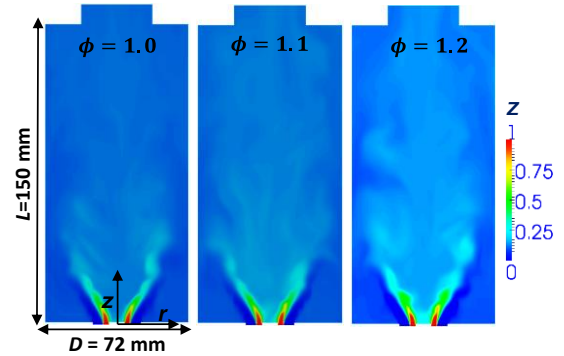


Figure 6. Mixture fraction distribution in non-premixed NH<sub>3</sub>/air flames in terms of overall  $\phi$

**Flame structures of the non-premixed flames:** Figure 5 elucidates temperature distributions of the non-premixed turbulent NH<sub>3</sub>/air flames at  $P_0 = 0.1$  MPa in terms of overall  $\phi$ , and there is a lower temperature region in the center region of the flame, unlike to the premixed flames. Moreover, central region temperature further decreases with the increase in overall  $\phi$ , and subsequently, flame was blow-off at the overall  $\phi = 1.25$ . This is possibly because of the much richer flame conditions in the central region of the flame as shown in Fig. 6 using the mixture fraction,  $Z$ , distributions. Here, mixture fraction was calculated based on the Bilger's mixture fraction equation and mixture fraction at the stoichiometric condition,  $Z_{st}$  is 0.142.

**NO emission characteristics of non-premixed flames:** Figures 7 and 8 show the NO and OH distributions of turbulent non-premixed NH<sub>3</sub>/air flames at  $P_0 = 0.1$  MPa in terms of the overall  $\phi$ , and it clearly shows that NO production is corresponded to the OH concentration. In non-premixed flames, NO production is depended on the local equivalence ratios of the flame region, and thus, there is a significant NO production in the lean flame regions around the wall boundaries owing to higher concentration of OH even in the overall-rich flame conditions. However in non-premixed flames also, similar to the premixed flames, NO emission decreases with the increase in overall  $\phi$ , and moreover, in high pressures (not shown here), NO emission decreases because of low OH concentration.

**Evaluation of effects of pressure on emissions of premixed and non-premixed flames:** NO emission decreases with the increase in  $\phi$  (or overall  $\phi$ ) and pressure irrespective to the combustion type, even though pressure impact was minimal for the  $\phi > 1.2$ , as shown in Figs. 9 and 10. Nevertheless, it is importantly observed that STAE of NO in non-premixed cases are slightly higher than that of the premixed cases at same  $\phi$ . This is possibly related to the local  $\phi$  variation in non-premixed cases. Moreover, in the all cases, unburnt NH<sub>3</sub> emission also reduces with an increase in pressure, and this is because of increase in the overall Damköhler Number. However, there is no effect of pressure on H<sub>2</sub> emission in both combustion types.

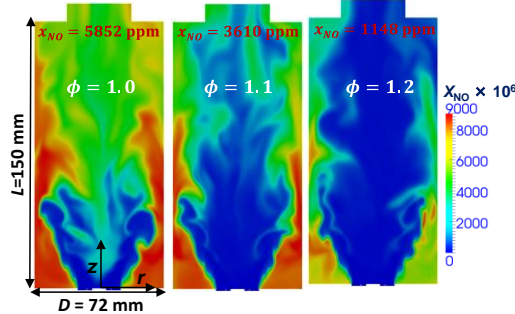


Figure 7. NO distributions of non-premixed NH<sub>3</sub>/air flames at  $P_0 = 0.1$  MPa in terms of overall  $\phi$

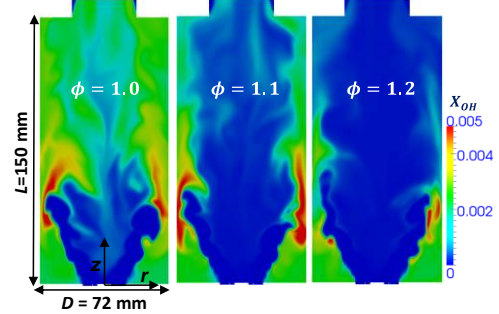


Figure 8. OH concentration of non-premixed NH<sub>3</sub>/air flames at 0.1 MPa in terms of overall  $\phi$

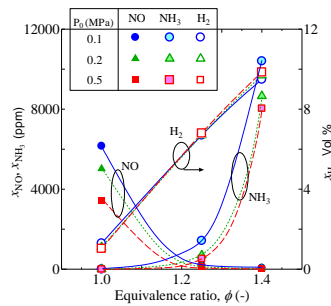


Figure 9. STAE of NO, NH<sub>3</sub>, and H<sub>2</sub> of NH<sub>3</sub>/air premixed flames in terms of  $P_0$  and  $\phi$

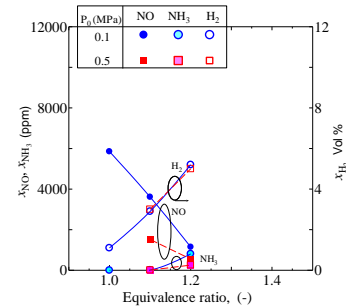


Figure 10. STAE of NO, NH<sub>3</sub>, H<sub>2</sub> of NH<sub>3</sub>/air non-premixed flames in terms of  $P_0$  and  $\phi$

## 4 Concluding remarks

In the present study, combustion and emission characteristics of premixed and non-premixed NH<sub>3</sub>/air flames were comprehensively numerically studied, and found that pressure effect is very significant on the NO reduction of NH<sub>3</sub>/air combustion. However, the STAE of NO in non-premixed flames are slightly higher than that of premixed cases. Moreover, the study verified that third body reaction of  $\text{OH} + \text{H} + \text{M} \rightleftharpoons \text{H}_2\text{O} + \text{M}$  plays significant role on the reduction of OH concentration, and thereby reduction of NO emissions.

## Acknowledgment

This research is supported by the Council for Science, Technology and Innovation (CSTI), the Cross-ministerial Strategic Innovation Promotion Program (SIP), “Energy Carriers” (Funding agency: The Japan Science and Technology Agency (JST)).

## References

- [1] Takizawa K, Takahashi A, Tokuhashi K, Kondo S, Sekiya A. (2008). Burning velocity measurements of nitrogen-containing compounds. *J. Hazard. Mater.* 155:144.
- [2] Hayakawa A, Goto T, Mimoto R, Arakawa Y, Kudo T, Kobayashi H. (2015). Laminar burning velocity and Markstein length of ammonia/air premixed flames at various pressures. *Fuel*. 159: 98.
- [3] Somarathne KDKA, Hayakawa A, Kobayashi H. (2016). Numerical investigation on the combustion characteristics of turbulent premixed ammonia/air flames stabilized by a swirl burner. *J. Fluid Sci. Tech.* 11: 16-00126.
- [4] Somarathne KDKA, Hatakeyama S, Hayakawa A, Kobayashi H. (2016). Numerical investigation on the emission reduction characteristics of the turbulent premixed ammonia/air flames stabilized by a swirl burner. *Proc. Japan Heat Transf. Sympo.* 53: I 212.
- [5] Hayakawa A, Arakawa Y, Mimoto R, Somarathne KDKA, Kudo T, Kobayashi H. (2017). Experimental investigation of stabilization and emission characteristics of ammonia/air premixed flames in a swirl combustor. *Int. J. Hydro. Energy*. In Press.
- [6] Kurata S, Iki N, Matsunuma T, Inoue T, Tsujimura T, Furutani H, Kobayashi H, Hayakawa A. (2017). Performances and emission characteristics of NH<sub>3</sub>-air and NH<sub>3</sub>-CH<sub>4</sub>-air combustion gas turbine power generations. *Proc. Combust. Inst.* 36:3351.
- [7] Regulatory Measures against Air Pollutants Emitted from Factories and Business Sites and the Outline of Regulation - Emission Standards for Soot and Dust, and NO<sub>x</sub> by Ministry of the Environment, Government of Japan. (1998). [https://www.env.go.jp/en/air/aq/air/air4\\_table.html](https://www.env.go.jp/en/air/aq/air/air4_table.html)
- [8] Duynslaegher C, Jeanmart H, Vandooren J. (2010). Ammonia combustion at elevated pressure and temperature conditions. *Fuel*. 89: 3540.
- [9] Hayakawa A, Goto T, Mimoto R, Kudo T, Kobayashi H. (2015) NO formation /reduction mechanisms of ammonia/air premixed flames at various equivalence ratios and pressures. *Mech. Eng. J.* 2:14-00402.
- [10] Nicoud F, Ducros F. (1999). Subgrid-scale stress modelling based on the square of the velocity gradient tensor. *J. Flow Turb. Combust.* 62: 183.
- [11] Miller JA, Smooke MD, Green RM, Kee RJ. (1983). Kinetic modeling of the oxidation of ammonia in flames. *Combust. Sci. Tech.* 34: 149.
- [12] Miller JA, Bowman CT. (1989). Mechanism and modeling of nitrogen chemistry in combustion. *Prog. Energy and Combust. Sci.* 15: 287.